

Measurement of the magnetic penetration depth of a superconducting MgB₂ thin film with a large intraband diffusivity

Jeehoon Kim,^{1,*} N. Haberkorn,¹ Shi-Zeng Lin,¹ L. Civale,¹ E. Nazaretski,² B. H. Moeckly,³
C. S. Yung,³ J. D. Thompson,¹ and R. Movshovich¹

¹Los Alamos National Laboratory, Los Alamos, New Mexico 87545, USA

²Brookhaven National Laboratory, Upton, New York 11973, USA

³Superconductor Technologies Incorporated, Santa Barbara, California 93111, USA

(Received 13 April 2012; revised manuscript received 12 June 2012; published 5 July 2012)

We report the temperature-dependent magnetic penetration depth $\lambda(T)$ and the superconducting critical field $H_{c2}(T)$ in a 500-nm MgB₂ film. Our analysis of the experimental results takes into account the two-gap nature of the superconducting state and indicates larger intraband diffusivity in the three-dimensional (3D) π band compared to that in the two-dimensional (2D) σ band. Direct comparison of our results with those reported previously for single crystals indicates that larger intraband scattering in the 3D π band leads to an increase of λ . We calculated λ and the thermodynamic critical field $H_c \approx 2000$ Oe by employing the gap equations for two-band superconductors. Good agreement between the measured and calculated λ value indicates the two independent measurements, such as magnetic force microscopy and transport, provide a venue for investigating superconducting properties in multiband superconductors.

DOI: [10.1103/PhysRevB.86.024501](https://doi.org/10.1103/PhysRevB.86.024501)

PACS number(s): 74.25.N-, 74.25.fc, 74.25.Ha, 74.25.Op

I. INTRODUCTION

During the past decade a significant effort has been made to understand the mechanism of two-band superconductivity in MgB₂.¹⁻⁴ MgB₂ has two *s*-wave gaps residing on four different disconnected Fermi surface (FS) sheets: two axial quasi-two-dimensional (2D) σ -band sheets and two contorted three-dimensional (3D) π -band sheets. The σ band forms two concentric cylindrical sheets via in-plane *sp*² hybridization of the boron valence electrons. The π band results from the strongly coupled covalent bonding and antibonding of the boron P_z orbitals.⁵ Multiple bands allow for both interband and intraband scattering. It is thus possible to tune the upper critical field (H_{c2}) via doping, which has different effects on the interband and intraband scattering strengths.^{2,6-8} In MgB₂ the anisotropy of the temperature-dependent penetration depth λ , $\gamma_\lambda(T) = \lambda_c(T)/\lambda_{ab}(T)$, shows remarkably different behavior compared to that of H_{c2} , $\gamma_{H_{c2}}(T) = H_{c2}^{ab}(T)/H_{c2}^c(T)$.^{9,10} This difference indicates that the two-band nature of superconductivity profoundly alters the superconducting properties compared to those in a single-band material.¹¹ For example, the equations for critical fields and depairing current as a function of λ and ξ should be modified due to the interband and/or intraband scattering. Knowledge of the absolute values of λ and ξ is also important for technological applications.¹² For example, the acceleration field in superconducting radio-frequency (SRF) cavities could be enhanced by covering conventional superconducting Nb cavities with superconductor/insulator multilayers (such as MgB₂) with a higher thermodynamic critical field (H_c).¹³

A number of measurements have been performed to determine the absolute value of λ in MgB₂.^{3,9,10} The reported values of λ range from 40 to 200 nm, indicating that λ is strongly affected by interband and intraband scattering.¹⁴⁻²⁰ In this paper we present measurements of the absolute values of $\lambda(T)$, employing low temperature magnetic force microscopy (MFM), and of the angular-dependent $H_{c2}(T, \theta)$ performed

via electrical transport, in a 500-nm-thick MgB₂ film. Our MgB₂ film can be described by the dirty limit two-band Usadel equations. We analyze the measured values of H_{c2} and λ using a model developed for dirty superconductors,² which simplifies the analysis compared to that reported in Ref. 15. We investigate theoretically the influence of the intraband scattering on the superconducting properties. Using a two-band superconductor model with parameters obtained from a fit to $H_{c2}(T, \theta)$, we calculate λ and H_c , which are consistent with the experimental values.

II. EXPERIMENT

A MgB₂ film was grown on a *r*-sapphire substrate by a reactive evaporation technique.^{21,22} The film is epitaxial and shows columnar growth morphology, with the *c* axis tilted by a few degrees from the normal direction of the substrate. For more details, see Ref. 22. The sample has dimensions $L = 4$ mm \times $W = 5$ mm \times $t = 500$ nm, and exhibits a full superconducting volume fraction based on measurements using a commercial superconducting quantum interference device (SQUID) magnetometer (Quantum Design magnetic property measurement system, MPMS) All MFM measurements described here were performed in a home-built low temperature MFM apparatus.²³ Temperature-dependent vortex images were taken in the frequency-modulated mode after a small magnetic field was applied above T_c (field cooled). We used high resolution SSS-QMFMR cantilevers.²⁴ The magnetic field was always applied perpendicular to the film surface and parallel to the MFM tip. The absolute values of $\lambda(T)$ were determined by comparing the Meissner response curves with those for a reference sample at 4 K.^{25,26} The Meissner technique for the λ measurement was first proposed by Xu *et al.*²⁷ and demonstrated by Lu *et al.*²⁸ The film thickness of 500 nm is larger than $\lambda \approx 200$ nm, which makes corrections to λ due to the sample thickness insignificant.

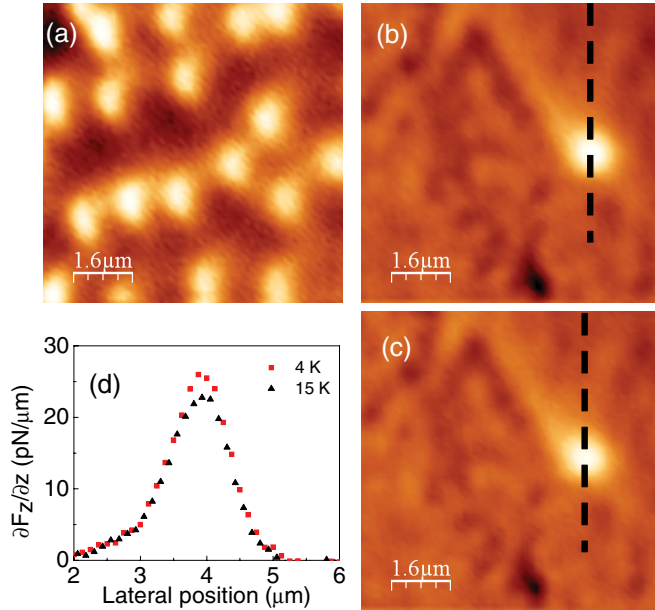


FIG. 1. (Color online) (a) A typical vortex image with a tip-lift height of 300 nm in the MgB_2 thin film. (b) and (c) Single vortex images with a tip-lift height of 300 nm, acquired at $T = 4$ K and $T = 15$ K, respectively. (d) The single vortex profile along the dotted lines in (b) and (c). A higher peak value corresponds to a smaller λ value.

Conventional four-lead resistivity measurements used for determining $H_{c2}(T, \theta)$, where θ is an angle between the applied magnetic \mathbf{H} and the crystallographic c axis, were performed with a rotatable probe in a commercial Quantum Design physical property measurement system (PPMS), in magnetic fields between 0 and 9 T. The superconducting critical temperature $T_c = 38.3$ K (zero resistance) and the transition width $\Delta T_c = 0.5$ K were determined from the transport measurements. Zero-field-cooling measurements at the MPMS with $H \approx 1$ Oe show $T_c = 38.0$ K. The small value of the residual resistivity ratio (RRR ≈ 4) indicates the presence of impurities, consistent with the dirty limit.

III. RESULTS AND DISCUSSION

A. MFM measurements in the MgB_2 film

Figure 1(a) presents a typical vortex image in the MgB_2 thin film. The well-formed vortices in the $6 \mu\text{m} \times 6 \mu\text{m}$ field of view were observed, which suggests the homogeneity of the sample on a micrometer scale. However, the irregular shape of individual vortices suggests the presence of inhomogeneity in the superfluid density on a submicrometer scale, which may be related to impurities. Figures 1(b) and 1(c) show MFM images of isolated vortices in MgB_2 at 4 and 15 K, respectively. The features besides a single vortex represent a submicrometer scale inhomogeneity, indicating small variations of superfluid density. Figure 1(d) depicts a line profile taken along the dotted line in Figs. 1(b) and 1(c) for each of the vortices. The maximum force gradient [$\max(\partial f/\partial z)$] at the center of the vortex qualitatively indicates that the magnitude of λ at 15 K is larger than that at 4 K.^{29–31} In order to determine

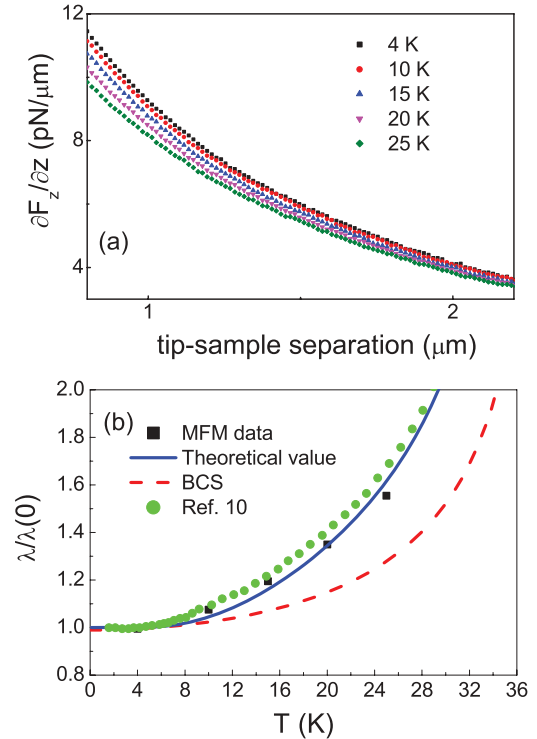


FIG. 2. (Color online) (a) Temperature dependence of the MFM Meissner response in MgB_2 . (b) $\lambda(T)$ marked by the black squares are inferred from the data shown in (a). The blue solid curve shows the calculated $\lambda(T)$ from the gap equations for two-band superconductors. The red dashed curve represents the conventional BCS model. The green circles are taken from tunnel diode resonator measurements (Ref. 10).

the absolute value of λ , we performed Meissner experiments. The force between the tip magnetic moment (a distance d above the sample) and the shielding currents induced by the tip field is equal to the force between the real tip and the image tip, with the mirror plane at a distance λ below the sample's surface.³² This force therefore is a function of $d + \lambda$ when $d \gg \lambda$. Direct comparison of the Meissner curves taken at 4 K for MgB_2 and a reference sample (Nb) with a known λ gives $\lambda(4 \text{ K}) = 200 \pm 30$ nm for MgB_2 .²⁵ Comparing Meissner curves for MgB_2 at 4 K and at a given temperature T yields $\delta\lambda(T)$. We obtain the absolute value of the temperature-dependent $\lambda(T)$ by adding $\delta\lambda(T)$ to $\lambda(4 \text{ K})$. Figure 2(a) shows the Meissner force response as a function of the tip-sample distance at several temperatures. The systematic evolution of the Meissner response with respect to temperature reflects the change of λ with temperature. Figure 2(b) shows the normalized $\lambda(T)$ (black squares) obtained for MgB_2 deviating significantly from the BCS theory curve (the red dashed line), which is consistent with the previous studies shown as green solid circles.¹⁰ This discrepancy indicates a profound effect of two-band superconductivity in MgB_2 .¹⁰ The large λ in MgB_2 may be due to inclusion of impurities, such as C, N, and Al, which significantly affects the electron mean free path in each band.

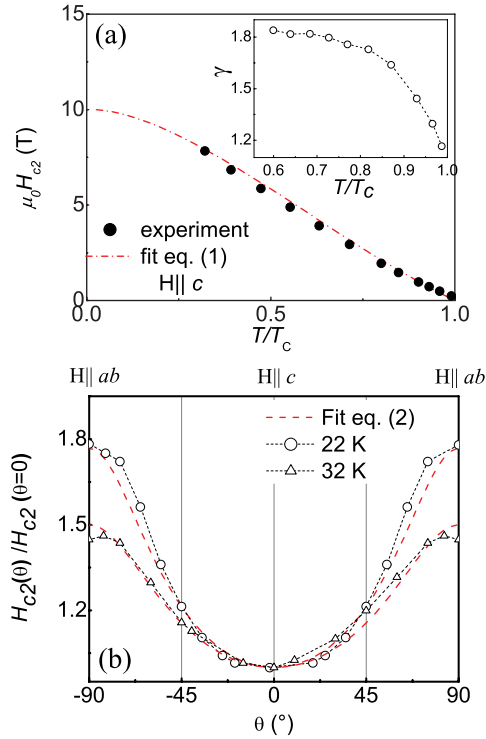


FIG. 3. (Color online) (a) Numerical fit to $H_{c2}(T)$ obtained from transport data. The inset shows the temperature dependence of the anisotropy of H_{c2} . (b) Numerical fit to $H_{c2}(\theta)$ at 22 and 32 K with the same parameters used to fit $H_{c2}(T)$. From the fit, the diffusivity values of $D_1^{ab} = 2.36 \text{ cm}^2/\text{s}$ and $D_2^{ab} = 19.7 \text{ cm}^2/\text{s}$ were obtained; the coupling parameters obtained from the fit are $L_{\sigma\sigma} \approx 0.810$, $L_{\pi\pi} \approx 0.285$, $L_{\sigma\pi} \approx 0.25$, and $L_{\pi\sigma} \approx 0.18$, respectively, close to the values obtained from *ab initio* calculations (Ref. 34). The uncertainty of the fit parameters is no more than 5%, which is smaller than our experimental errors of 10%.

B. H_{c2} measurements in the MgB₂ film

In order to investigate the nature of disorder, we performed temperature-dependent H_{c2} measurements. Figure 3(a) shows $H_{c2}(T)$ with the field parallel to the c axis $H_{c2}^{\parallel c}(T)$ (black circles). The value of $H_{c2}(0)$ is considerably higher than that found in clean single crystals ($H_{c2}^{\parallel c}(0) \approx 3\text{--}5 \text{ T}$),³³ which indicates that the film is in the dirty limit. The Gurevich model for two-band superconductors² considers interband and intraband scattering by nonmagnetic impurities in the dirty limit. The high T_c in our film (which shows essentially no suppression compared to the clean crystals) is consistent with a small interband scattering, so we can use the equations obtained for $H_{c2}(T)$, neglecting the interband scattering:

$$a_2[\ln(t) + U(\eta h)] + a_1[\ln(t) + U(h)] + a_0[\ln(t) + U(h)][\ln(t) + U(\eta h)] = 0, \quad (1)$$

where $U(x) = \psi(1/2 + x) - \psi(1/2)$, $\psi(x)$ is the digamma function, $a_1 = 1 + L_-/L_0$, $a_2 = 1 - L_-/L_0$, $a_0 = 2w/L_0$, $L_0 = \sqrt{(L_-^2 + 4L_{12}L_{21})}$, $L_{\pm} = L_{11} \pm L_{22}$, $w = L_{11}L_{22} - L_{12}L_{21}$, $t = T/T_c$, $\eta = D_2/D_1$, and $h = H_{c2}D_1/2\Phi_0T$. Φ_0 is a single magnetic flux quantum, and D_1 and D_2 are the intraband diffusivities. The angular-dependent diffusivities $D_1(\theta)$ and $D_2(\theta)$ for both bands are calculated using the

following equation:

$$D_m(\theta) = \sqrt{D_m^{(a)2} \cos^2 \theta + D_m^{(a)} D_m^{(c)} \sin^2 \theta}. \quad (2)$$

From Eqs. (1) and (2), we can obtain $H_{c2}(T, \theta)$.

The diffusivity D_1^c along the c axis is smaller than the in-plane diffusivity D_1^{ab} in MgB₂ due to the nearly 2D nature of the σ band. On the other hand, the values of D_2^c and D_2^{ab} do not differ substantially because of the isotropic 3D nature of the π band. The resulting relations among diffusivities are $D_1^c \ll D_1^{ab}$ and $D_2^c \approx D_2^{ab}$, which leads to the anomalous behavior of the anisotropy of $H_{c2}(T)$. The in-plane diffusivity ratio D_1^{ab}/D_2^{ab} is an important parameter in Eq. (1).

We performed a numerical fit to three sets of transport data such as $H_{c2}(T)$ at $\theta = 0^\circ$, $H_{c2}(\theta)$ at $T = 22 \text{ K}$, and $T = 32 \text{ K}$ using Eqs. (1) and (2), shown in Fig. 3. The relation between the best fit intraband diffusivities in the σ and π bands is $D_2^a = 8.5D_1^a$. This large $\eta = 8.5$ is consistent with the absence of a sharp upward curvature in $H_{c2}^{\parallel c}(T)$ at low T (see Fig. 1 in Ref. 2), frequently observed in C-doped MgB₂ with extremely high H_{c2} . The inset of Fig. 3(a) shows the anisotropy $\gamma_{H_{c2}}(T)$ as a function of T . Again, this behavior is qualitatively consistent with that expected for $\eta \gg 1$ [see Fig. 3(c) in Ref. 2]. The superconducting critical field $H_{c2}^{\parallel c}(0)$ for field applied parallel to the c axis, obtained from the fit, equals 10 T. This indicates the presence of strong multiple intraband scattering channels. The value of the in-plane intraband diffusivity ratio $\eta = 8.5$ provides information about the type of intraband scatterers. The larger value of η (smaller value of D_1^a) indicates the weakening of the 2D σ band by certain types of impurities, such as C and N. These impurities affect the 2D landscape by replacing p_{xy} orbitals of boron, and making the system more isotropic. The large value of D_2^a compared to D_1^a is also in good agreement with results from the α model,¹⁰ and is the result of a large contribution of the π band to the total density of states.

C. λ and H_c from the two-band model

We calculated λ using the parameters obtained from the $H_{c2}(T, \theta)$ fit and the band calculations. The London equation for a two-gap superconductor is given by $\nabla \times (\lambda_L^2 \nabla \times \mathbf{H}) + \mathbf{H} = 0$, where the London penetration depth is $\lambda_L^{-2}(T) = \pi e^2 \mu_0 (N_1 D_1^{ab} \Delta_1 \tanh \frac{\Delta_1}{2T} + N_2 D_2^{ab} \Delta_2 \tanh \frac{\Delta_2}{2T})$: Indices of 1 and 2 represent the σ band and the π band, respectively. N_1 and N_2 are the electron densities of states. Δ_1 and Δ_2 are the gap magnitudes. D_1^{ab} and D_2^{ab} are the intraband diffusivities.² Using $D_1^{ab} = 2.36 \text{ cm}^2/\text{s}$, $D_2^{ab} = 19.7 \text{ cm}^2/\text{s}$, obtained from the fit of $H_{c2}(T, \theta)$, $\Delta_1(0) = 84 \text{ K}$, $\Delta_2(0) = 33 \text{ K}$, obtained from the gap Eqs. (3), $N_1 = 0.3 \text{ states}/a^3 \text{ eV}$, and $N_2 = 0.41 \text{ states}/a^3 \text{ eV}$ with a unit cell volume of $a^3 = 87.2 \text{ \AA}^3$ (Ref. 14) (obtained from the band calculations),³⁴ we obtain $\lambda_L(0) \approx 170 \text{ nm}$, consistent with the measured value of $\lambda_{ab}(0) = 200 \pm 30 \text{ nm}$. The calculated $\lambda_L(T)$ is shown as the blue curve in Fig. 2(b), consistent with the MFM experiment. This indicates that the two independent measurements of $\lambda(T)$ (MFM) and $H_{c2}(T)$ (transport) in MgB₂ are complementary for investigating superconducting properties.

The thermodynamic critical field (H_c) in MgB₂ is important for technological applications.¹² We evaluate H_c using the

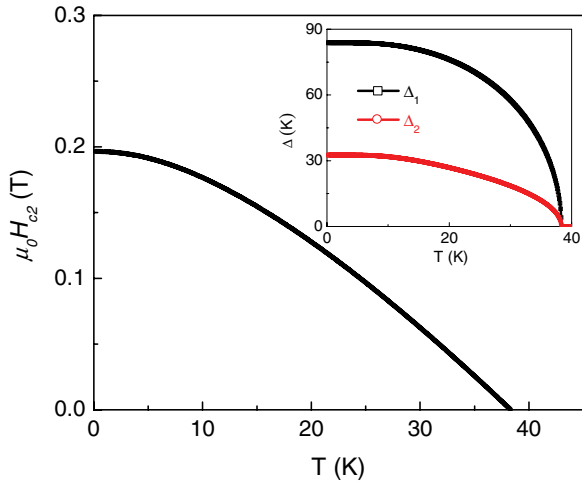


FIG. 4. (Color online) The calculated thermodynamic critical field H_c from the gap equations for two-band superconductors. The inset shows the calculated gap values from the two band model.

band coupling parameters, obtained from $H_{c2}(T, \theta)$, and the electron density of states obtained from the band calculations. The gap equations for two-band superconductors³⁵ are

$$\hat{g} \begin{pmatrix} \Delta_1 \\ \Delta_2 \end{pmatrix} - \begin{pmatrix} N_1(0)\Delta_1 Y(\Delta_1) \\ N_2(0)\Delta_2 Y(\Delta_2) \end{pmatrix} = 0, \quad (3)$$

with $Y(\Delta_j) = \int_0^{\omega_c} d\xi \frac{1}{\sqrt{(\xi^2 + |\Delta_j|^2)}} \tanh\left[\frac{\sqrt{\xi^2 + |\Delta_j|^2}}{2k_B T}\right]$, where \hat{g} is the superconducting coupling matrix with $g_{11} = N_1 L_{22}/w$, $g_{12} = g_{21} = N_1 L_{12}/w = N_2 L_{21}/w$, and $g_{22} = N_2 L_{11}/w$. ω_c is some unknown cutoff frequency obtained from Eqs. (3) using the T_c obtained from the transport data. Using the parameters obtained from the fit of $H_{c2}(T, \theta)$, we have the superconducting coupling matrix $\hat{g} = \begin{pmatrix} 0.46 & -0.40 \\ -0.40 & 1.78 \end{pmatrix} / (a^3 \text{ eV})$. The free energy is calculated³⁵ as $\mathcal{F} = \sum_{ij} (\Delta_i g_{ij} \Delta_j^*) - \frac{4}{\beta} \sum_i N_i \int_0^{\omega_c} d\xi \ln\left(\frac{\cosh(\frac{1}{2}\beta\sqrt{|\Delta_i|^2 + \xi^2})}{\cosh(\frac{1}{2}\beta\xi)}\right)$. Then H_c is given by $H_c^2/8\pi = -\mathcal{F}$. We calculate $\Delta_1(T)$ and $\Delta_2(T)$ as shown in Fig. 4 (inset). The calculated gap values at zero temperature are $\Delta_1(0) = 84$ K and $\Delta_2(0) = 33$ K, which are slightly larger than reported values.¹⁰ The thermodynamic critical field at zero temperature, calculated from the two-band model, is approximately 2000 Oe. This value is smaller than those

previously obtained in polycrystalline MgB_2 by specific heat measurements³⁶ and the values reported in clean single crystals.^{37,38}

As discussed earlier, the superconducting properties in multiband superconductors are affected by the interactions among the bands.³⁷ We obtain $\xi_{ab}(0) = 5.7$ nm using $H_{c2}(0) = \Phi_0/2\pi\xi^2(0)$ and our experimental value $H_{c2}^{\parallel c}(0) = 10$ T. We can then use the Ginzburg-Landau theory to estimate the thermodynamic critical field in the film, $H_c = \Phi_0/2\sqrt{2}\pi\lambda(0)\xi(0) = 2100 \pm 300$ Oe. This value is close to the calculated value of $H_c = 2000$ Oe from the two-band model. This suggests that the strong intraband scattering in the 3D π band makes the system more isotropic, and thus the system shows single band characteristics.

IV. CONCLUSION

In conclusion, we have measured $\lambda_{ab}(T)$ and $H_{c2}(T, \theta)$ in a MgB_2 film. Our analysis of $H_{c2}(T, \theta)$ shows that the large value of the in-plane intraband diffusivity in the 3D π band is due to the presence of nonmagnetic impurities such as C and N, indicating the system is more isotropic, which is partly responsible for a large λ . We calculated λ and H_c by employing the gap equations for the two-band superconductors using the parameters obtained from $H_{c2}(T, \theta)$ and derived from band calculations. The calculated $\lambda_L(0) \approx 170$ nm is close to the measured $\lambda(0) = 200 \pm 30$ nm, indicating that two independent measurements, such as MFM and transport, are complementary, and provide a venue for thoroughly investigating superconducting properties. The determination of $H_c(T)$ in clean MgB_2 and in multiband superconductors in general is a fascinating problem with both fundamental and technological relevance.

ACKNOWLEDGMENTS

We acknowledge valuable discussions and communication of data with A. Gurevich. Work at Los Alamos (all measurements, data analysis, manuscript preparation) was supported by the US Department of Energy, Basic Energy Sciences, Division of Materials Sciences and Engineering. Work at Brookhaven (manuscript preparation) was supported by the US Department of Energy under Contract No. DE-AC02-98CH10886. N.H. is member of CONICET (Argentina).

*Corresponding author: jeehoon@lanl.gov

¹J. Nagamatsu, N. Nakagawa, T. Maranaka, Y. Zenitani, and J. Akimitsu, *Nature (London)* **410**, 63 (2001).

²A. Gurevich, *Phys. Rev. B* **67**, 184515 (2003).

³V. G. Kogan, C. Martin, and R. Prozorov, *Phys. Rev. B* **80**, 014507 (2009).

⁴U. Welp, A. Rydha, G. Karapetrov, W. K. Kwok, G. W. Crabtree, C. Marcenat, L. M. Paulius, L. Lyard, T. Klein, J. Marcus, S. Blanchard, P. Samuely, P. Szabo, A. G. M. Jansen, K. H. P. Kim, C. U. Jung, H.-S. Lee, B. Kang, and S.-I. Lee, *Physica C* **385**, 154 (2003).

⁵P. Samuely, P. Szabo, J. Kacmarcik, T. Klein, and A. G. M. Jansen, *Physica C* **385**, 244 (2003).

⁶B. J. Senkowicz, J. E. Giенcke, S. Patnaik, C. B. Eom, E. E. Hellstrom, and D. C. Larbalestier, *Appl. Phys. Lett.* **86**, 202502 (2005).

⁷A. Matsumoto, H. Kumakura, H. Kitaguchi, B. J. Senkowicz, M. C. Jewell, E. E. Hellstrom, Y. Zhu, P. M. Voyles, and D. C. Larbalestier, *Appl. Phys. Lett.* **89**, 132508 (2006); A. Serquis, G. Serrano, M. S. Moreno, L. Civale, B. Maiorov, F. Balakirev, and M. Jaime, *Supercond. Sci. Technol.* **20**, L12 (2007).

⁸V. Braccini *et al.*, *Phys. Rev. B* **71**, 012504 (2005).

- ⁹V. G. Kogan, *Phys. Rev. B* **66**, 020509(R) (2002).
- ¹⁰J. D. Fletcher, A. Carrington, O. J. Taylor, S. M. Kazakov, and J. Karpinski, *Phys. Rev. Lett.* **95**, 097005 (2005).
- ¹¹M. Tinkham, *Introduction to Superconductivity* (McGraw-Hill, New York, 1975).
- ¹²E. W. Collings, M. D. Sumption, and T. Tajima, *Supercond. Sci. Technol.* **17**, S595 (2004).
- ¹³A. Gurevich, *Appl. Phys. Lett.* **88**, 012511 (2006).
- ¹⁴X. X. Xi, *Rep. Prog. Phys.* **71**, 116501 (2008).
- ¹⁵A. A. Golubov, A. Brinkman, O. V. Dolgov, J. Kortus, and O. Jepsen, *Phys. Rev. B* **66**, 054524 (2002), and references therein.
- ¹⁶T. Dahm and D. J. Scalapino, *Appl. Phys. Lett.* **85**, 4436 (2004).
- ¹⁷X. K. Chen, M. J. Konstantinović, J. C. Irwin, D. D. Lawrie, and J. P. Franck, *Phys. Rev. Lett.* **87**, 157002 (2001).
- ¹⁸K. H. Lee, K. H. Kang, B. J. Mean, M. H. Lee, and B. K. Cho, *J. Magn. Magn. Mater.* **272**, 165 (2004).
- ¹⁹F. Simon *et al.*, *Phys. Rev. Lett.* **87**, 047002 (2001).
- ²⁰D. K. Finnemore, J. E. Ostenson, S. L. Bud'ko, G. Lapertot, and P. C. Canfield, *Phys. Rev. Lett.* **86**, 2420 (2001).
- ²¹B. H. Moeckly and W. S. Ruby, *Supercond. Sci. Technol.* **19**, L21 (2006).
- ²²L. Gu, B. H. Moeckly, and D. J. Smith, *J. Cryst. Growth* **280**, 602 (2005).
- ²³E. Nazaretski, K. S. Graham, J. D. Thompson, J. A. Wright, D. V. Pelekhov, P. C. Hammel, and R. Movshovich, *Rev. Sci. Instrum.* **80**, 083074 (2009).
- ²⁴A SSS-QMFMR cantilever, Nanosensors, Inc., [www.nanoandmore.com/USA/AFM-Probe-SSS-QMFMR.html]
- ²⁵J. Kim, L. Civale, E. Nazaretski, N. Haberkorn, F. Ronning, A. S. Sefat, T. Tajima, B. H. Moeckly, J. D. Thompson, and R. Movshovich, [arXiv:1206.4525](https://arxiv.org/abs/1206.4525).
- ²⁶J. Kim, F. Ronning, N. Haberkorn, L. Civale, E. Nazaretski, N. Ni, R. J. Cava, J. D. Thompson, and R. Movshovich, *Phys. Rev. B* **85**, 180504(R) (2012).
- ²⁷J. H. Xu, J. H. Miller, and C. S. Ting, *Phys. Rev. B* **51**, 424 (1995).
- ²⁸Q. Lu, K. Mochizuki, J. T. Markert, and A. de Lozanne, *Physica C* **371**, 146 (2002).
- ²⁹O. M. Auslaender, L. Luan, E. W. J. Straver, J. E. Hoffman, N. C. Koshnick, E. Zeldov, D. A. Bonn, R. Liang, W. N. Hardy, and K. A. Moler, *Nat. Phys.* **5**, 35 (2009).
- ³⁰E. W. J. Straver, J. E. Hoffman, O. M. Auslaender, D. Rugar, and K. A. Moler, *Appl. Phys. Lett.* **93**, 172514 (2008).
- ³¹T. Shapoval, H. Stopfel, S. Haindl, J. Engelmann, D. S. Inosov, B. Holzapfel, V. Neu, and L. Schultz, *Phys. Rev. B* **83**, 214517 (2011).
- ³²L. Luan, O. M. Auslaender, T. M. Lippman, C. W. Hicks, B. Kalisky, J. H. Chu, J. G. Analytis, I. R. Fisher, J. R. Kirtley, and K. A. Moler, *Phys. Rev. B* **81**, 100501(R) (2010).
- ³³G. K. Perkins, J. Moore, Y. Bugoslavsky, L. F. Cohen, J. Jun, S. M. Kazakov, J. Karpinski, and A. D. Caplin, *Supercond. Sci. Technol.* **15**, 1156 (2002).
- ³⁴A. A. Golubov, J. Kortus, O. V. Dolgov, O. Jepsen, Y. Kong, O. K. Andersen, B. J. Gibson, K. Ahn, and R. K. Kremer, *J. Phys.: Condens. Matter* **14**, 1353 (2002).
- ³⁵S.-Z. Lin and X. Hu, *Phys. Rev. Lett.* **108**, 177005 (2012).
- ³⁶Y. X. Wang, T. Plackowski, and A. Junod, *Physica C* **355**, 179 (2001).
- ³⁷F. Bouquet, R. A. Fisher, N. E. Phillips, D. G. Hinks, and J. D. Jorgensen, *Phys. Rev. Lett.* **87**, 047001 (2001).
- ³⁸M. Zehetmayer, M. Eisterer, J. Jun, S. M. Kazakov, J. Karpinski, A. Wisniewski, and H. W. Weber, *Phys. Rev. B* **66**, 052505 (2002).